XV International Conference on Durability of Building Materials and Components
DBMC 2020, Barcelona
C. Serrat, J.R. Casas and V. Gibert (Eds)

Evaluation of Pore Structure of Hardened Cement Paste Immersed in Sodium Sulfate Solution

Otsuka Sakata, H. Nicolas [1], Kennosuke Sato[2] and Shigehiko Saito[2]

[1] University of Yamanashi, Faculty of Engineering, Integrated Graduate School of Medicine, Engineering and Agricultural Sciences, 4-3-11, Takeda, Kofu, Yamanashi, 400-8511, Japan, g19tc003@yamanashi.ac.jp

[2] University of Yamanashi, Graduate School of Engineering, Department of Civil Engineering and Environmental Engineering, 4-3-11, Takeda, Kofu, Yamanashi, 400-8511, Japan, satok@yamanashi.ac.jp

Abstract. *The purpose of the present study is to evaluate pore structure of hardened cement paste immersed in sodium sulfate solutions and to experimentally examine the relation between the change of pore structure and hydration products. Cement paste specimens were immersed in sodium sulfate solutions and ion-exchanged water for two weeks. Since oxygen gas can pass through the pores having micro scale, it is possible to evaluate the effect of the pore structure on the oxygen transport in cement pastes. Thus, the oxygen diffusion coefficient (D_{O2}) of the specimens after immersion were measured, and the pore volume and the pore size distribution were also measured. In addition, the phase compositions of the specimens were acquired. As a result, D_{O2} of the specimens immersed in the sodium sulfate solutions decreased as compared to the specimens immersed in the ion-exchanged water. The tortuosity of the specimens immersed in the sodium sulfate solutions increased due to decreasing of the pore volume having a diameter larger than 20 nm. There was a correlation between the volume of ettringite and the pore volume having a diameter larger than 20 nm. According to the above results, it was considered that the decreasing of D_{O2} in the case of sulfate immersion can occur as a result of the complication of the pore structure owing to filling of the pores by ettringite.*

Keywords: *Sulfate Attack, Oxygen Diffusion Coefficient, Pore Structure, Tortuosity, Ettringite.*

1 Introduction

The sulfate attack is known as a chemical reaction caused by sulfate and causes the fragility and tissue fragility in hardened cement paste by generating a large amount of ettringite. Although there are not many cases of sulfate deterioration in Japan, there is a high potential risk of sulfate attack in Japan because it is revealed that the marine clay layer producing sulfates is widely distributed (Matsushita *et al.*, 2010). In addition, it is considered that cement-based materials are used for building of radioactive waste processing facilities.

Generally, in order to predict the deterioration phenomenon, it is necessary to grasp the ion transfer characteristics affecting the degradation of hardened cement paste. Furthermore, the ion transfer in the hardened cement paste is known to be greatly affected by the pore structure. Thus, in order to predict the progress of sulfate attack, it is necessary to grasp the pore structure as a transferring field of sulfate ions. However, the pore structure and mass transfer characteristics are significantly changed when the sulfate ions penetrate the hardened cement paste. Sulfate ions causes a reaction with cement hydrate constituting the solid phase and generates ettringite in large quantities, that is considered the cause of change, but there are few

examples of experimentally examined changes of pore structure and mass transfer characteristics when affected by sulfate attack.

Therefore, we evaluated the oxygen transfer characteristics affected solely by pore structure to clarify the change in the pore structure of the hardened cement paste immersed in sodium sulfate solutions.

2 Specimens and Methods

2.1 Preparation of Specimens

In this study, ordinary portland cement was used. Table 1 shows the chemical compositions of the cement, and Table 2 shows the density and specific surface area. The mineral compositions calculated by Bogue equation is shown in Table 3. Three types of cement paste specimens having water to cement ratio of 45%, 55% and 65% were prepared. The size of the specimens was 3 × 4 × 0.5 cm. It was demolded at 1 d, and it was wet-sealed curing until 28 d at 20 °C.

Table 1. Chemical compositions of cement (mass%).

Ig. loss	insol.	SiO_2	Al_2O_3	Fe_2O_3	CaO	MgO
0.71	0.08	20.89	5.44	2.94	65.11	1.54

Na_2O	K_2O	TiO_2	P_2O_5	MnO	Cl	Total
0.27	0.53	0.26	0.14	0.05	0.014	97.99

Table 2. Density and surface area of cement.

Density (g/cm^3)	Blaine specific surface area (cm^2/g)
3.16	3450

Table 3. Mineral compositions of cement (mass%).

C_3S	C_2S	C_3A	C_4AF	Gypsum	MgO
60.00	15.00	9.00	9.00	3.54	1.54

2.2 Sodium Sulfate Immersion and Ion-Exchanged Water Immersion

The specimens were immersed in sulfate solutions. Sodium sulfate and ion-exchanged water (electrical conductivity 0.055μS/cm) were used for sulfate solutions. The concentrations of sodium sulfate solutions were 0.5 and 5 mass%. The specimens were immersed in solutions with the liquid-to-solid ratio of 5.0 at 20 °C for 2 weeks. The specimens were also immersed in the ion-exchanged water for comparison with the case of sodium sulfate immersion.

2.3 Analysis

The pore volume of each specimen was measured by Archimedes method. Each specimen after immersion was crushed into small pieces, after which 3 pieces (about 3 g) were immersed in ion-exchanged water and reduced pressure for 30 min. The mass of the specimens under water and the mass of the surface-dried condition were subsequently measured. Thereafter, the specimens were dried at 50 °C in a drying oven until the specimens mass no longer changed. The pore volume was calculated by the following equation (1)

$$V = \frac{m_s - m_{50d}}{m_s - m_W} \tag{1}$$

where V is the pore volume (m^3/m^3), m_s is the mass of the surface-dried condition (g), m_{50d} is the mass of the dried condition at 50 °C (g), and m_w is the mass of the specimen under water(g).

Pore size distribution was measured by mercury-intrusion-porosimeter. The crushed samples (about 5 mm) were immersed in acetone for 2 d to prevent further hydration. These specimens were subsequently placed under vacuum to remove the acetone and stored in a desiccator in the presence of silica gel until the mass no longer changed. The pressure range was 0.1 kPa to 400MPa. The measurement range of the pore diameter is approximately 4 nm to 120 μm.

Kikuchi *et al*. (2010) was measured the oxygen diffusion coefficient of the hardened cement paste, which is capable of grasping the complexity of the pore structure. Therefore, in order to grasp the pore structure of the specimens immersed in sodium sulfate solutions, the oxygen diffusion test was performed. The specimens after immersion were dried in a desiccator containing silica gel until the mass no longer changed. The oxygen diffusion test was carried out with reference to the method of Shirakawa *et al*. (1999). The oxygen concentration was recorded, when the change in oxygen concentration in the nitrogen gas side cell became constant. The oxygen diffusion coefficient was determined using the formula (2)

$$D_{O_2} = \frac{R_N \cdot (C_N - C_b) \cdot (L + \delta_N + \delta_O)}{\left\{1 - \frac{R_N}{R_O} \cdot \left(\frac{M_O}{M_N}\right)^{\frac{1}{2}} \cdot (C_N - C_b) - C_N\right\} \cdot A_C} \tag{2}$$

where D_{O_2} is the oxygen diffusion coefficient (cm^2/s), C_N is the oxygen concentration in nitrogen gas (%), C_b is the oxygen concentration in nitrogen gas cylinder (%), R_N and R_O are the nitrogen and oxygen gas flow rates (cm^2/s), M_N and M_O are the nitrogen and oxygen molecular weight (g/mol), L is the specimen thickness (cm), A_C is the cross-sectional area of the specimen (cm^2), and δ_N and δ_O are the boundary film thickness of the nitrogen gas side and oxygen gas side (mm).

Phase composition of the crystal phase of the sample was quantified by XRD / Rietveld analysis. The samples after immersion were immersed in acetone for 2 d and subsequently placed under vacuum to remove the acetone for 2 d. The samples were crushed and dried at 20 °C and 11% RH until the sample mass no longer changed. In this study, corundum was used as a standard sample, and the amount of the amorphous phase was quantified by the external standard method (Sagawa *et al.*, 2014). The compositions of amorphous phase and CaO/SiO_2 molar ratio of C-S-H (C/S ratio) were calculated by mass balance calculation (Maruyama *et al*., 2010) using the composition of each hydrate in 11% RH reported by Suda *et al*. (2014).

3 Results and Discussion

3.1 Effect of Sodium Sulfate on Oxygen Diffusion Coefficient

Figure 1 shows the oxygen diffusion coefficient of the sample immersed in sodium sulfate and ion-exchanged water. The oxygen diffusion coefficients of the specimens immersed in sodium

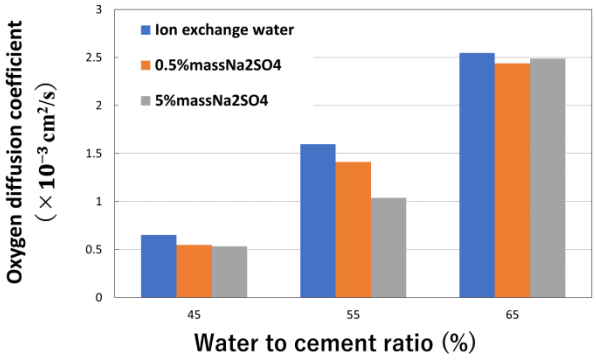

Figure 1. Oxygen diffusion coefficient of hardened cement pastes after immersion.

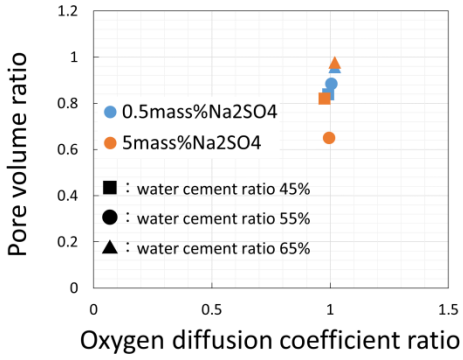

Figure 2. Relationship between oxygen diffusion coefficient ratio and pore volume ratio.

sulfate were reduced regardless of the water-to-cement ratio as compared with the case of ion-exchanged water. However, the degree of decreasing in the oxygen diffusion coefficient varies from water-to-cement ratio. The water-to-cement ratio 55% is large reduction degree, on the other hand, the degree of decreasing was reduced at the water-to-cement ratio 65%.

3.2 Change in Pore Structure by the Effects of Sodium Sulfate

The relationship between the decreasing in the oxygen diffusion coefficient affected by sodium sulfate and the change in the pore structure of the specimens was examined. First, the effect of the change in the pore volume was examined to quantify the change caused by the effect of sodium sulfate. The oxygen diffusion coefficient ratio R_{O_2} was calculated by the equation (3) using the value of the sample immersed in ion-exchanged water $D_{O_2\_water}$, which is not affected by sodium sulfate. Similarly, the pore ratio was calculated.

$$R_{O_2} = \frac{D_{O_2\_Na_2SO_4}}{D_{O_2\_water}} \tag{3}$$

Figure 2 shows the relationship between the oxygen diffusion coefficient ratio and the pore volume ratio. From the figure, the pore volume ratio is almost unchanged at 1.0 while the oxygen diffusion coefficient ratio is greatly changed in the range of 1.0 to 0.6. Thus, the decreasing in the oxygen diffusion coefficient caused by the effect of sodium sulfate could not be explained by a change in the pore volume.

Because it has been reported that the tortuosity is an index representing the complexity of the pore structure (Saeki *et al.*, 2014), the tortuosity of the oxygen diffusion in the hardened cement paste was calculated in this study. The tortuosity of the oxygen diffusion was calculated using the formula (4), with reference to the past studies (Kikuchi *et al.*, 2010; Saeki *et al.*, *2014*)

$$D_{O_2} = \frac{1}{{\tau_{O_2}}^2} \cdot D \tag{4}$$

where τ_{O_2} is the tortuosity of the oxygen diffusion, and D is the effective diffusion coefficient in the pore (cm^2/s).

In this study, the parallel pore model was adopted, and the effective diffusion coefficient in the pore was calculated by equation (5)

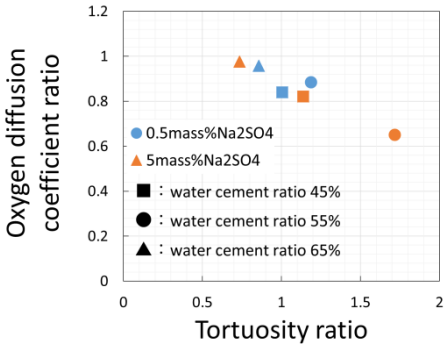

Figure 3. Relationship between oxygen diffusion coefficient ratio and tortuosity ratio.

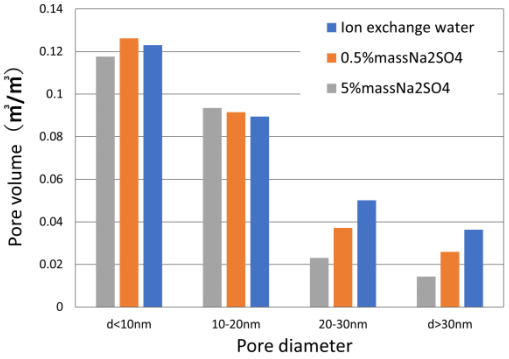

Figure 4. Pore volume of each pore diameter (water to cement ratio of 45%).

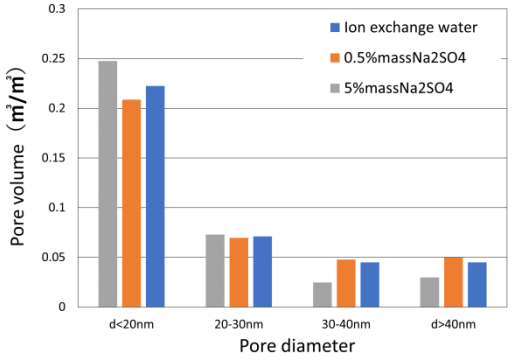

Figure 5. Pore volume of each pore diameter (water to cement ratio of 55%).

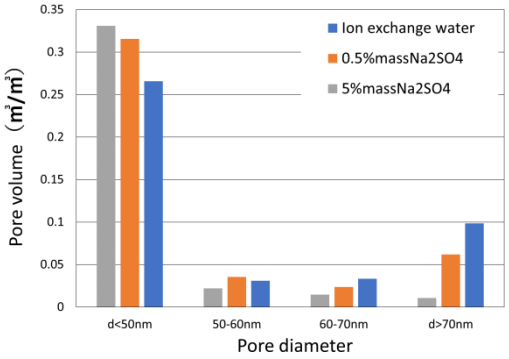

Figure 6. Pore volume of each pore diameter (water to cement ratio of 65%).

$$D = \left(\frac{\varepsilon_a}{\frac{1}{D_{Ka}} + \frac{1}{D_{ON}}} \right) + \left(\frac{\varepsilon_b}{\frac{1}{D_{Kb}} + \frac{1}{D_{ON}}} \right) \quad (5)$$

where ε_a is the pore volume having a diameter < 50 nm (cm^3/cm^3), ε_b is the pore volume having a diameter > 50 nm (cm^3/cm^3), D_{Ka} is the Knudsen diffusion coefficient of the average pore diameters < 50 nm (cm^2/s), D_{Kb} is the Knudsen diffusion coefficient of the average pore diameters > 50 nm (cm^2/s), D_{ON} is the molecular diffusion coefficient of nitrogen and oxygen (cm^2/s). The tortuosity ratio was calculated in the same manner as the oxygen diffusion coefficient ratio described above.

Figure 3 shows the relationship between the oxygen diffusion coefficient ratio and the tortuosity ratio. The oxygen diffusion coefficient ratio is reduced with increasing of the tortuosity ratio. These results suggest that the decreasing of the oxygen diffusion characteristics in the hardened cement paste affected sodium sulfate was caused by the increasing of the complexity of the pore structure due to sodium sulfate immersion.

Subsequently, in order to investigate the increasing of the pore structure complexity, we focused on changes in the pore size distribution. Figure 4 to 6 shows the pore volume of each

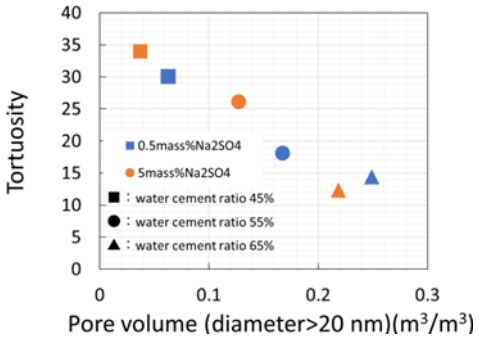

Figure 7. Relationship between tortuosity and pore volume (d > 20nm).

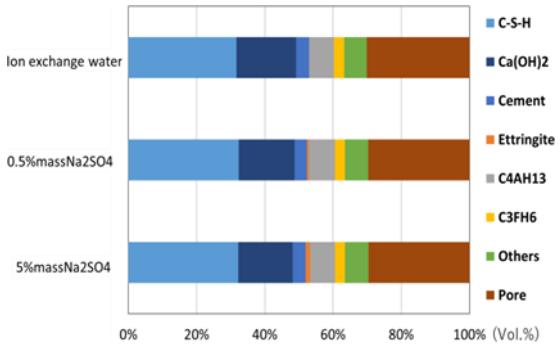

Figure 8. Phase compositions of the specimens after immersion (water-to-cement ratio of 45%)

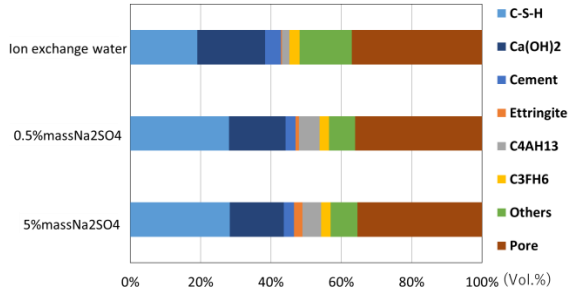

F igure 9. Phase compositions of the specimens after immersion (water-to-cement ratio of 55%)..

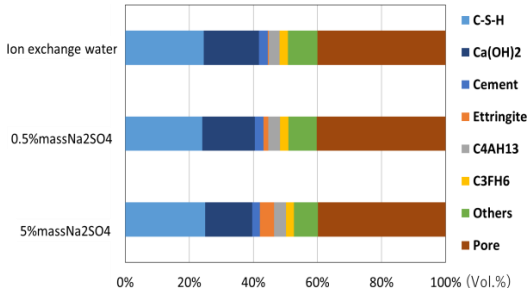

Figure 10. Phase compositions of the specimens after immersion (water-to-cement ratio of 65%).

pore diameter. From Figure 4, in the case of water-to-cement ratio of 45%, in the division of the diameter < 20nm, it was confirmed that the pore volume of the sodium sulfate immersion sample was slightly larger than that of the ion-exchanged water immersion sample. On the other hand, in the division of diameter > 20nm, the pore volume of the sodium sulfate immersion sample is reduced as compared to the ion-exchanged water immersion sample. It was confirmed that the diameter of 20 nm is the boundary of the trend change.

Figure 7 shows the relationship between the tortuosity and the pore volume having a diameter > 20 nm. From the figure, the tortuosity increased with decreasing of the pore volume having a diameter > 20nm. These results suggest that because the pore volume having a diameter > 20 nm in the specimen immersed in sodium sulfate decreased, the pore structure was complicated and the oxygen transfer was suppressed.

3.3 Effect of Hydration Products on the Change of Pore Structure

Figures 8 to 10 shows the phase compositions of the specimens after immersion having each water-to-cement ratio. In the case of the ion-exchanged water immersion, which is not affected by sodium sulfate, the C-S-H occupies most of the solid phases. In the case of sodium sulfate immersion, the C-S-H also occupies most of the solid phase at any water-to-cement ratio. Furthermore, the higher the water-to-cement ratio and the higher the sodium sulfate concentration, the amount of ettringite was increased. Therefore, we examined the relationship

between the pore volume having a diameter > 20 nm and the generation of C-S-H and ettringite.

In order to calculate the volume of C-S-H, which is affecting the pore volume, the amount of C-S-H was calculated using equation (6)

$$M_{C-S-H} = m_C \cdot \left(\frac{m'_{C-S-H}}{100}\right) \tag{6}$$

where M_{C-S-H} is the amount of C-S-H per unit volume (g/m^3), m_C is the amount of cement paste per unit volume (g/m^3), m'_{C-S-H} is the amount of C-S-H (cm^2/s). The volume of C-S-H V_I (m^3/m^3) was calculated by dividing the M_{C-S-H} by ρ_{C-S-H}, which is the density of C-S-H (g/m^3) as shown in equation (7).

$$V_I = \left(\frac{M_{C-S-H}}{\rho_{C-S-H}}\right) \tag{7}$$

Because the density of C-S-H changes depending on the C/S ratio, it was calculated from each C/S ratio using the equation (8) of Suda *et al*. (2014).

$$\rho_{C-S-H} = 0.45(C/S) + 1.36 \tag{8}$$

Furthermore, as shown in the equation (9), the volume of C-S-H was calculated

$$V_{C-S-H} = \frac{V_I}{P} \tag{9}$$

where V_{C-S-H} is the volume of C-S-H (m^3/m^3), P is the capillary pore volume (m^3/m^3).

Figure 11 shows the relationship between the C-S-H volume and the pore volume having a diameter > 20 nm. In both of the sodium sulfate solution concentration, the pore volume having a diameter > 20 nm decreased with the increasing of the volume of C-S-H. However, when a regression line was drawn for each sodium sulfate solution concentration, there was a slight error between the two lines. Since different linear relationships were shown for each solution concentration, it was considered that there were other factors besides the volume change of C-S-H in the change of the pore volume having a diameter > 20 nm. Therefore, the volume of ettringite was considered, in addition to C-S-H.

The volume of ettringite (V_{Ett}) was calculated using the same calculation as in equations (6), (7), and (9). The density of the ettringite was 1.78×10^6g/m^3 (Suda *et al*., 2014). As shown in equation (10), the total volume (V_{C-S-H_Ett}) was obtained by adding the V_{Ett} to the V_{C-S-H}.

$$V_{C-S-H\_Ett} = V_{C-S-H} + V_{Ett} \tag{10}$$

Figure 12 shows the relationship between the pore volume having a diameter > 20 nm and the volume of C-S-H and ettringite. In this case, the regression line drawn for each sodium sulfate solution concentration showed almost no error. These results suggest that the decreasing of the oxygen diffusion coefficient of the specimens affected by sodium sulfate was caused by the formation of ettringite, which is filling the pores having a diameter > 20 nm and the complication of the pore structure.

4 Conclusions

The purpose of this study was to investigate the effect of sodium sulfate on the oxygen transfer characteristics and the pore structure of hardened cement paste. The conclusions derived from this study can be summarized as follows.

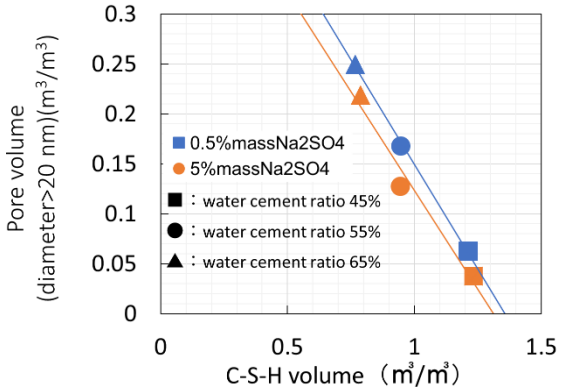

Figure 11. Relationship between pore volume (d > 20nm) and volume of C-S-H.

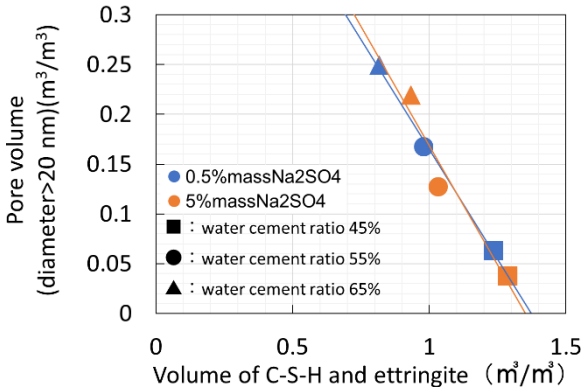

Figure 12. Relationship between pore volume (d > 20nm) and volume of C-S-H and ettringite.

When the cement paste was affected by sodium sulfate, the oxygen diffusion coefficient decreased compared to the case immersed in ion-exchanged water.

The decreasing of the oxygen diffusion coefficient affected by sodium sulfate was due to the increasing of the tortuosity owing to the decreasing of the pore volume having over 20 nm in diameter.

The decreasing of the oxygen diffusion coefficient of the specimens affected by sodium sulfate was caused by the formation of ettringite, which is filling the pores having over 20 nm in diameter and the complication of the pore structure.

ORCID

Herly Nicolas Otsuka Sakata: https://orcid.org/0000-0003-0434-9595
Kennosuke Sato: http://orcid.org/0000-0002-3456-4037
Shigehiko Saito: http://orcid.org/0000-0001-6789-3198

References

Maruyama, I., Matsushita T., Noguchi, Takafumi., Hosokawa, Y. and Yamada, K. (2010). *Rate of Hydration of Alite and Belite in Portland Cement -Hydration system of Portland cement Part 1-*. J. Struct. Constr. Eng., AIJ. 650, 681-688.

Matsushita, H., Sagawa, Y. and Sato, T. (2010). *Classification of probability of deterioration of concrete by sulfate arrack based on investigation results of sulfate content of ground.* Journal of Japan Society of Civil Engineers E, 66(4), 507-519.

Kikuchi, M., Suda, Y. and Saeki, T. (2010). *Evaluation for Ion Transport in Hardened Cementitious Paste by Oxygen Diffusion and Chloride Diffusion.* Cement Science and Concrete Technology, 64 346-353.

Shirakawa, T., Shimazoe, Y., Aso, M., Nagamatsu, S. and Sato, Y. (1999). *The Proposal of Testing Method for Determination of Gas Diffusion Coefficient in Hardenend Cement.* J. Struct. Constr. Eng., AIJ. 515, 15-21.

Sagawa, T. and Toyoharu, N. (2014). *Hydration Analysis and Phase Composition of Cement-based Materials by X-Ray Diffraction / Rietveld Method using an External Standard.* Cement Science and Concrete Technology, 68, 46-52.

Saeki, T., Mashima K., Kikuchi, M. and Saito, T. (2014). *Chroride Ion Diffusivity in Hardended Cementitious Materials using Various Silica Fume.* Cement Science and Concrete Technology, 68, 352-359.

Suda, Y., Saeki, T. and Saito, T. (2014). *Effect Chemical Composition of C-S-H on Volume and Pore Size Distribution of Gel Pore*. (2014). Journal of Japan Society of Civil Engineers E2, 70(2), 134-152.